Talanta 134 (2015) 30–36

Contents lists available at ScienceDirect

Talanta

journal homepage: www.elsevier.com/locate/talanta

Diagnostic applications of gastric carcinoma cell aptamers in vitro and in vivo

Fei Ding [a,1], Shan Guo [a,1], Min Xie [a,1], Wei Luo [b], Chunhui Yuan [b], Weihua Huang [a], Yan Zhou [c], Xiao-Lian Zhang [b,*], Xiang Zhou [a,**]

[a] College of Chemistry and Molecular Sciences, Key Laboratory of Biomedical Polymers of Ministry of Education, Wuhan University, Wuhan 430072, Hubei, PR China
[b] School of Medicine, Wuhan University, State Key Laboratory of Virology, Wuhan 430072, Hubei, PR China
[c] Zhongnan Hospital of Wuhan University, Wuhan 430072, Hubei, PR China

ARTICLE INFO

Article history:
Received 18 June 2014
Received in revised form
23 September 2014
Accepted 28 September 2014
Available online 30 October 2014

Keywords:
Aptamer
Cell-SELEX
Capture efficiency
Aptamer probe
Cancer imaging

ABSTRACT

Gastric carcinoma is the most malignant tumor. Due to lacking of efficient means to diagnose the cancer at the early stage, it is necessary to develop effective molecular probes for early diagnosis and treatment. We have selected aptamers with high specificity and affinity against SGC7901 cells by cell-SELEX (Systematic Evolution of Ligands by Exponential Enrichment) method, which shown important clinical applications: (1) Specific recognize human gastric tumor tissues compared to the normal tissues. (2) When used to capture cancerous cells, the aptamer-functionalized fluorescent-magnetic nanospheres (FMNS) could specifically capture 93% target cancer cells and about70% target cells can be released. (3) The aptamer probe displayed a quenched fluorescence in the absence of target cancer cells and went through a conformational transformation upon binding to target cancer cells that induced fluorescence. (4) The aptamer probe could target gastric tumors transplanted into mice with obvious fluorescence. The newly generated aptamers hold great potential in early cancer diagnosis.

1. Introduction

Human gastric carcinoma is the most common type of malignant tumors [1], it is important to develop cancer-specific and more sensitive methods.

In recently years, a new type of ligand called aptamer has shown great potential in molecular recognition and targeting [2,3]. Aptamers are evolved through an in vitro selection strategy called cell-SELEX (systematic evolution of ligands by exponential enrichment) from a DNA or RNA library [4–9]. Aptamers are short sequences of nucleotides, such as single-stranded DNA (ssDNA), RNA and modified nucleic acids. These nucleotides can be chemically synthesized and, site-specifically labeled, and therefore site-specifically immobilized. Moreover, because aptamers are much more hydrophilic than antibodies, they may not exhibit nonspecific binding [10].

Due to the rapid development of nanotechnology in science and technology today, its applications has increasingly widespread, the optical properties of nano-materials for the detection of biomolecular have gradually embarked on the stage. The reports are increasing based on magnetic nanoparticles for detection molecules. İsmail Hakkı Boyaci et al. [11] reported the use of antibody coated magnetic nanoparticles for *Escherichia coli* enumeration, this SERS-based sandwich immunoassay possessed a rapid and sensitive feature to target organisms with low detection limit and less detection time. Ramanaviciene et al. [12] reported the use of magnetic gold nanoparticles (MNP-Au) modified by antibodies in oriented or random manner were used for the binding of gp51, enhanced Raman scattering (SERS) was applied as detection method, this immunoassay was successfully applied for the detection of gp51 in milk samples in a rapid, reliable and selective manner.

Since the aptamers have many advantages in used as molecular probes, including low cost of synthesis, high binding affinity and specificity, tunbility and biocompatibility [13–16]. Therefore, aptamers have attracted a great deal of attention for used as biomarkers for cancer diagnosis and treatment. Tan's group developed the

* Corresponding author.
** Corresponding author at: College of Chemistry and Molecular Sciences, Key Laboratory of Biomedical Polymers of Ministry of Education, State Key Laboratory of Virology, Wuhan University, Wuhan 430072, Hubei, PR China.
Fax: +86 27 87336380.
E-mail addresses: zhangxiaolian@whu.edu.cn (X.L. Zhang), xzhou@whu.edu.cn (X. Zhou).
[1] These authors contributed equally to this work.

http://dx.doi.org/10.1016/j.talanta.2014.09.036
0039-9140/

cell-SELEX strategy to generate a panel of aptamers that can specifically distinguish between any two types of cell lines, more importantly, their newly generated aptamer probes can be used for the molecular profiling of cancer [17–20]. There also have reports on aptamers selected against human gastric tumors [21]. However, until now, the application of aptamers for medical use has been limited due to the scarcity of relevant and practical aptamers. Sreevatan et al. [22] reported the chemical synthesis and functionalization of magnetic and gold-coated magnetic nanoparticles to detect prion protein that was a target to a specific biotinylated aptamer, this study setted the stage for the development of prion detection platforms as well as elucidation the structure at the binding interface.

Because an aptamer selected against cancer cells can specifically bind target proteins of the cancer cells, the aptamer can be designed as a probe to recognize cancer cells in vivo and achieve cancer imaging with high specificity [23]. In the context of molecular imaging, many aptamer probes have been developed [24–26]. However, the same mechanism is not useful when attempting to design an aptamer that can be activated (aptamer-based activas probes) by a certain target [27]. Because aptamer probe sequences can be custom-designed, they can alter their conformation in the presence of the target and in turn transform into signal changes [28]. Based on this concept, the main aim of this study is to develop a series of effective aptamers and apply them to the study of human liver cancer in vitro.

In this report, we used a paired noncancer liver cell line and cancer liver cell line to perform Cell-SELEX. A human gastric cancer cell line, SGC7901cells, as a target and a normal human gastric mucosal cells, GES-1 cell, as a control. We performed the selection process at physiological temperature (37 °C) so that the cells and their membrane receptors were in its biologically active states and generated a panel of new aptamers that can recognize SGC7901cells with high specificity (Kd value in the low nanomolar range) and selectivity (differentiated target cancer cells from other non-targeted cells). We also demonstrated the potential of aptamer in clinical applications. The selected aptamers can specifically recognise human gastric tumor tissues compared to normal tissues. Moreover, when the selected aptamers were used to capture cancerous cells, it showed excellent capture and release efficiency. Based on its secondary structure, we designed an activatable fluorescent aptamer probe to generate a FRET effect in living cancer cells and achieved contrast-enhanced cancer visualization in vitro. In vivo studies demonstrated that activated fluorescence signals were obviously achieved in the SGC7901 tumor sites in mice.

2. Materials and methods

2.1. Cell lines and buffers

SGC7901cell (human gastric adenocarcinoma cells), HeLa cell (human cervical carcinoma cells), A498cell (Human renal cell carcinoma cells), and HT29 cell (Human colon adenocarcinoma cells) were obtained from American Type Culture Collection., and cultured in MEM medium supplemented with 10% FBS GIBCO) and 100 units/ml penicillin–streptomycin (Beyotime), GES-1 cell (Human gastric epithelial cells), MDA-MB-231 cell (Human breast cancer cells) were obtained from American Type Culture Collection, and cultured in DMEM medium contained 10% FBS (GIBCO) and 100 units/ml penicillin–streptomycin (Beyotime). Washing buffer contained 4.5 g/L glucose and 5 mM $MgCl_2$ in Dulbecco's PBS (Hyclone). Binding buffer was prepared by adding 1 mg/mL

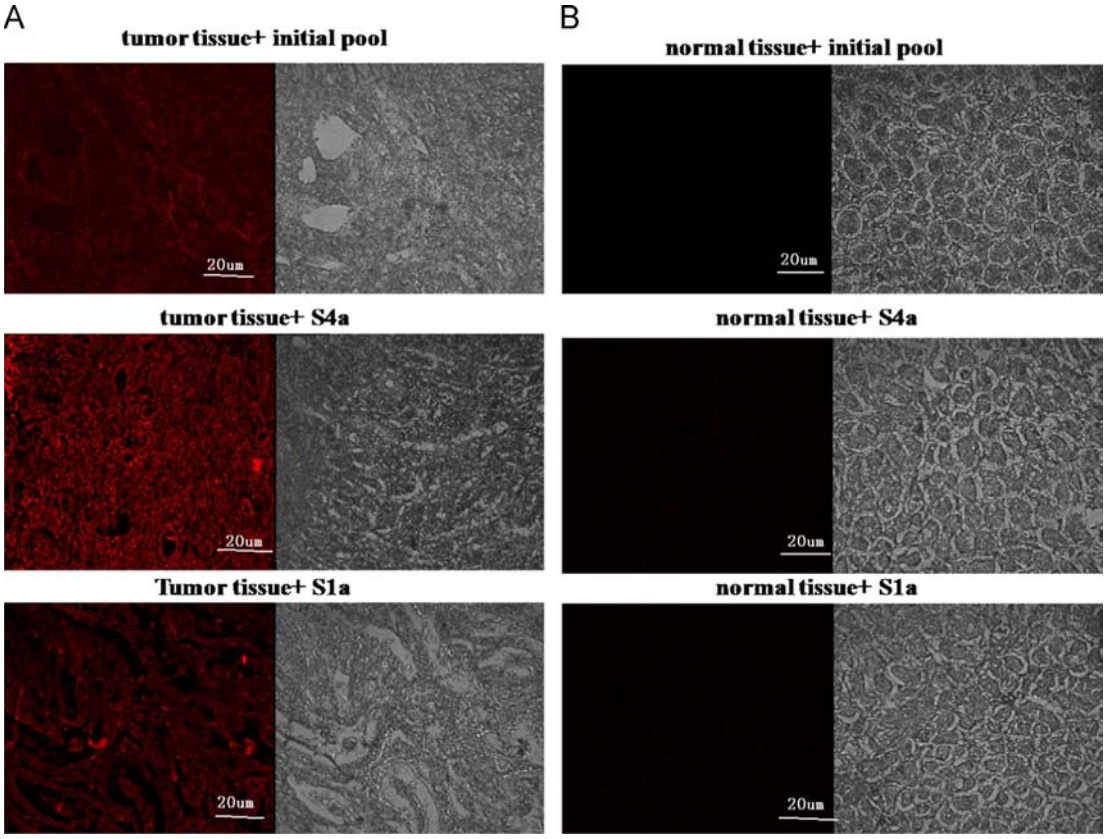

Fig. 1. Confocal images and optical images of formalin-fixed gastric tumor sections (A) and normal gastric sections (B) embedded in paraffin were stained by aptamers S1a and S4a labeled with Cy5 and BHQ2. In each picture, left column is the fluorescent images and right column is the optical images, respectively. (For interpretation of the references to color in this figure legend, the reader is referred to the web version of this article.)

BSA, 0.1 mg/mL yeast tRNA and 15% fetal bovine serum into the washing buffer to reduce background binding. All the DNA sequences used in this article were custom-designed and then synthesized by Takara Bio Inc. Trypsin and proteinase K were purchased from Fisher Biotech.

2.2. Animal

Male athymic BALB/c (Balb/c-nu) mice were obtained from the Wuhan University ABSL-III Laboratory. They were 3 weeks old at the start of each experiment and weighed about 12 g. All animal operations were in accord with institutional animal use and care regulations, approved by the Laboratory Animal Center of Hunan.

2.3. Tissues

Human gastric tumor tissues and human normal gastric tissues were obtained from Zhongnan Hospital of Wuhan University, School of Medicine.

2.4. Ethics statement

This study was carried out in strict accordance with the recommendations in the Guide for the Care and Use of Laboratory Animals of the National Institutes of Health. The protocol was approved by the Committee on the Ethics of Animal Experiments of the University of Wuhan University ABSL-Ⅲ Laboratory. All surgery was performed under sodium pentobarbital anesthesia, and all efforts were made to minimize suffering.

2.5. Confocal imaging of human tissues stained with aptamer

Human gastric tumor tissues and normal tissues were formalin-fixed and embedded in paraffin. Five micrometer sections were cut from each paraffin block for microscopic examination. The 5-μm sections were first dewaxed, and then incubated with Cy5 labeled-aptamers (300 nM) in binding buffer containing 15% FBS at 37 °C for 20 min. After washing, the slides were examined under excitation at

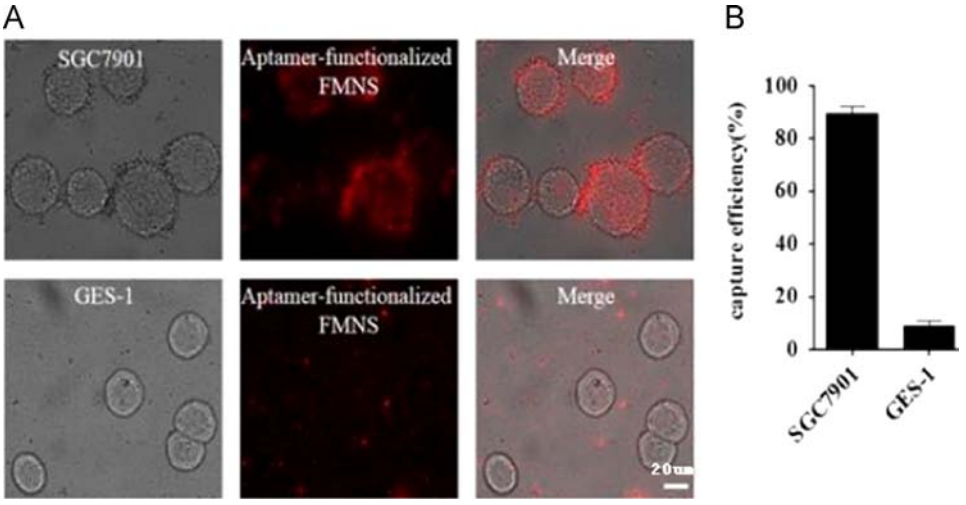

Fig. 2. Specific recognition and capture of SGC7901 cells using aptamer-functionalzied FMNS. Microscopic images of SGC7901 cells incubated with aptamer-functionalized FMNS at 37 °C for 15 min followed by magnetic attraction (top); GES-1 cells incubated with aptamer-functionalized FMNS without magnetic attraction as control (bottom). Bright field: left column; fluorescent image: middle column; merged image: right column (A) and capture capability of aptamer-functionalized FMNS to the cells (mean ± SD; $n=5$(B)).

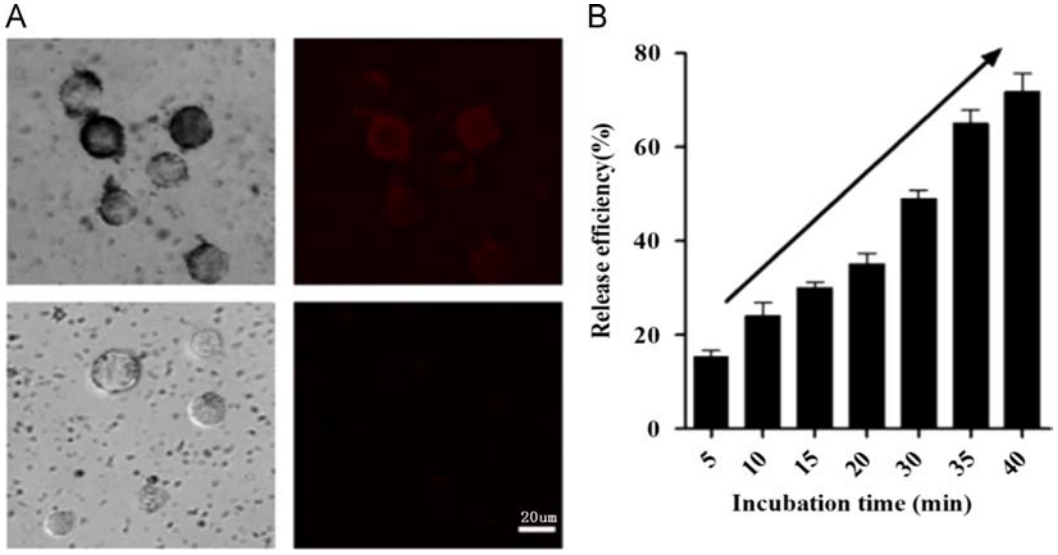

Fig. 3. Target cells release assay. Microscopic images of SGC7901 cells incubated with aptamer-functionalized FMNS followed by magnetic attraction (top); SGC7901 cells were released with benonase nuclease cleaved aptamers after magnetic attraction (bottom). Bright field: left column; fluorescent image: right column (A) and time-dependent release efficiency for SGC7901 cells (mean ± SD; $n=5$(B)).

630 nm by confocal imaging (20 × objective) (Nikon C1-si TE2000, Japan).

2.6. Cell capture assay

To demonstrate the capture specificity of aptamer-functionalized FMNSs to targeted cells, SGC7901 cells (3×10^5) were used as positive cells, While GES-1 cells (3×10^5) were used as a negative control. Briefly, cells were detached from the flask using trypsin-EDTA solution, and collected by centrifugation at 800 rpm for 6 min at room temperature. Next, the cells were washed twice with 1 × PBS and suspended in D'PBS buffer. Aptamer-functionalized FMNSs were dispersed in 60 μL of D'PBS and incubated with cell suspension (440 μL) on an orbital shaker for 15 min at 37 °C. After attraction for 5 min on magnetic separation device (MagnaBot® 96 Magnetic Separation Device, Promega), the SGC7901 cells were isolated and imaged by fluorescent microscope. While GES-1 cells incubated with aptamer-functionalized FMNS were observed directly without magnetic isolation. The capture capacity of aptamer-functionalized FMNSs to SGC7901 cells were detected. First, SGC7901 cells were incubated with aptamer-functionalized FMNSs followed by magnetic separation. Subsequently, the uncaptured SGC7901 cells were counted to calculate the capacity efficiency of aptamer-functionalized FMNSs to SGC7901 cells. Meanwhile, GES-1 cells were used as control to evaluate whether aptamer-functionalized FMNS has non-specific interaction with GES-1 cells.

2.7. Fabrication of aptamer-functionalized fluorescent-magnetic multifunctional nanospheres (FMNS)

Carboxylated poly(styrene/acrylamide) copolymer nanospheres were synthesized by a modified emulsion-free method [29]. Trioctylphosphine oxide capped CdSe/ZnS quantum dots were purchased from Jiayuan Quantum Dots (QDs) Corporation (Wuhan, China). Nano-γ-Fe_2O_3 particles were prepared from the reaction of ferricacetylacetonate, HDA, and oleic acid [30]. Nano-γ-Fe_2O_3 paticles, QDs and ethanol-dehydrated nanopsheres were mixed and swelled in a chloroform/butanol solvent (5: 95 vol/vol) and then ultrasonicated for at least 30 min. To remove free nano-γ-Fe_2O_3 and QDs, the mixture was dispersed in *n*-hexane and centrifuged for 1 min at 5000 rpm. In the end, the FMNSs were washed with ethanol for several times and well dispersed in water. After attraction by magnetic scaffold, the isolated nanospheres were kept in boric acid buffer (10 mM, pH = 7.4).

Subsequently, streptavidin-conjugated FMNSs were obtained by incubation of streptavidin with FMNSs in the presence of 9 mM of 1-ethyl-3-(3-dimethylaminopropyl) carbodiimide hydrochloride (EDC) on ice in for 4 h. The extra streptavidin was removed and final product was stocked in PBS for later use. To verify whether streptavidin was successfully conjugated with FMNS, 12 μL of biotin-FITC (50 μg/mL) was incubated with 100 μL of streptavidin-conjugated FMNS or pure FMNS for 1 h, respectively. After removing surplus biotin-FITC, biotin-FITC pre-incubated streptavidin-conjugated FMNSs or pure FMNSs were kept in 1 × PBS for imaging (pH = 7.2).

To fabricate aptamer-functionalized FMNSs, biotinylated aptamer (0.8 μM, Invitrogen) was incubated with streptavidin-conjugated FMNSs at room temperature for 1 h. The biotinylated aptamer was immobilized on streptavidin-conjugated FMNS via biotin–streptavidin interaction.

2.8. Flow cytometry assays with fluorescent aptamer probes

Generally, fluorescent aptamer probes were incubated with 3×10^5cells in 300 μL binding buffer at 37 °C for 15 min in the dark and then immediately injected and determined with a FACScan cytometer (BD Biosciences) by counting 20,000 events. Especially for the detection sensitivity assay, different amounts of SGC7901 cells were stained by 300 nM activatable fluorescent aptamer probe in 200 μL binding buffer at 37 °C in the dark. After incubation for 15 min, the samples were immediately detected with flow cytometer by counting the aptamer probes-labeled events appearing in the upright (UR) region.

2.9. In vivo specific cancer imaging with fluorescent aptamer probes

Three-week-old male BALB/c nude mice received a subcutaneous injection of 1×10^7 in vitro-propagated cancer cells into the backside below right costal margin. Tumors were then allowed to grow for 7 to 10 days. Before imaging, BALB/c nude mice with tumors were anesthetized with the anesthetic. In detail, an intraceliac injection was performed with 100 mg/kg dose of pentobarbital sodium solution. Once the mice were anesthetized to be motionless, a 100 μL volume of PBS (pH = 7.4) containing 1.5 nmol of labeled aptamer probe and 4.5 nmol unselected pool were injected intravenously via the tail vein. At specified times, fluorescence images of the dorsal side of live mice were taken by a Maestro™ in vivo fluorescence imaging system (Cambridge Research & Instrumentation, Inc.). A 640 nm (± 25 nm) band pass filter and a 680 nm long pass filter were selected to be used as the excitation filter and the emission filter, respectively. All the fluorescence images were presented after processing by the Image J software (version 1.38x).

3. Results and discussion

Here we first selected a group of aptamers against human gastric cancer cells via cell-SELEX strategy shown in Fig. S1[31], the detailed SELEX procedures were shown in the Supporting information. Sequences and Kds of selected aptamers and its corresponding truncated lengths [32] for gastric cancer were shown in Table S1, the secondary structures of aptamers and its truncated aptamers were shown in Fig. S2. All of the teuncated aptamers had very high specificity and binding affinity for the target cells, SGC7901 cells, but did not bind with the control, GES-1 cells or other non-target cells (the results were shown in Supplementary information Fig. S3 and Table S2). And we also studied the likely target for aptamers (results are shown in Supplementary information Fig. S4 and Table S3).

Then, we first applied the aptamers to detect clinical samples of human gastric tumor tissues and normal human gastric tissues. The aptamer S1a and S4a were designed with the Cy5 fluorophore at the 5′ end and the quencher group BHQ2 at the 3′ end. Aptamer was incubated with formalin-fixed human gastric tumor tissues and normal human gastric tissues embedded in paraffin. As shown in Fig. 1, tumor tissues gave bright red fluorescence after incubation with Cy5-labelled aptamer S1a and S4a, while negligible fluorescent signal was observed from formalin-fixed normal gastric tissue sections stained with Cy5-labelled S1a and S4a. This results clearly verified that the selected aptamers were highly specific for gastric tumor cells, and that they did not bind to cells in normal gastric tissues. This observation further showed the potential of aptamers as specific molecular probes for gastric cancer analysis.

To show that the selected aptamers could be used for CTCs capture, target cell capture (SGC7901) and release assays using the selected aptamer was performed. GES-1 cell line was used as the control to study nonspecific binding. The aptamer S4a was modified as follows: 5′-biotin-GATCTCTCTCTGCCCTAAGTCC GCACCCGTGCTTCCCTGT-3′. Here we used aptamer-functionalized fluorescent-magnetic nanospheres (FMNs) as a capture scaffold, the FMN was coated with streptavidin, so our biotin-labeled aptamer could be attached to it (the detail synthesized procedures of the FMNs were shown in experimental

section, and the features of FMN were shown in Fig. S5). From Fig. 2A we could find that the SGC7901 cells were clustered by large number of aptamer-functionalized FMNS, while the control cells, GES-1 cells, were not captured by aptamer-functionalized FMNS, so nearly no fluorescence was observed on the cell surface. Fig. 2B shown the clear differences of the cell number on aptamer-founctionalized substrates. After magnetic attraction, we calculated the cells numbers captured by aptamer-functionalized FMNS, accounting for a capture efficiency of 93% for positive cells (SGC7901 cells), in contrast, only less than 7% of control cells were captured.

While for target cells release, with benzonase nuclease (EMD, 25 U/mL, 2 U) treatment, nearly most of the FMNs were detached from the SGC7901 cells, so very faint fluorescence was observed (Fig. 3A up line). Fig. 3B summarized the release efficiency increased with increasing incubation time of aptamer-FMNs-SGC7901cells complex in the benzonase nuclease, about 70%

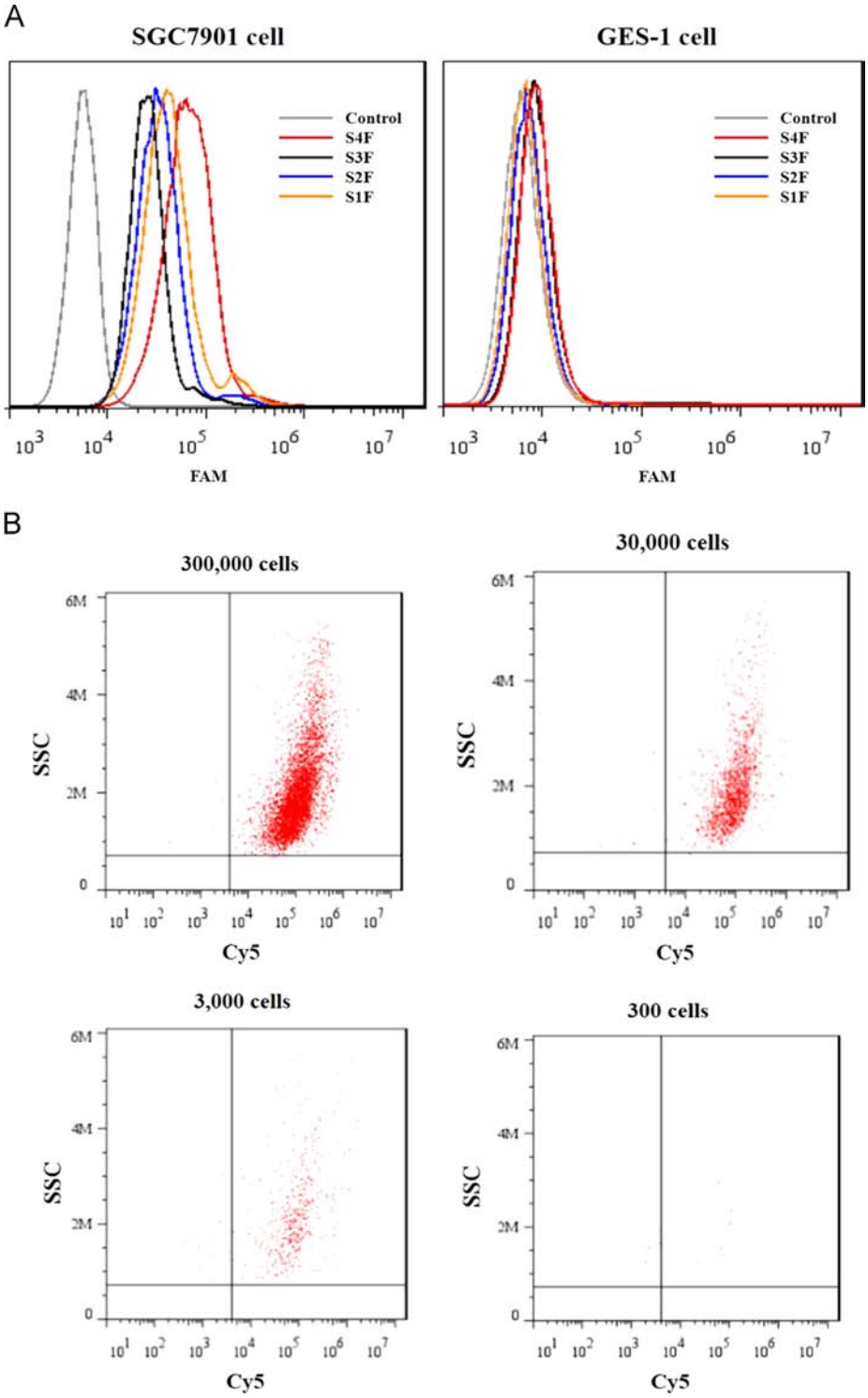

Fig. 4. Flow cytometry assays of SGC7901 cells and GES-1 cells after incubation with the fluorescent aptamer probe FAM-S1F-BHQ1, FAM-S2F-BHQ1, FAM-S3F-BHQ1 and FAM-S4F-BHQ1, respectively. The flow cytometry assays were performed by counting 30,000 events, and the used concentration of the probes was 250 nM (A). Flow cytometry assays of SGC7901 cells with decreasing cell amounts in 200 μL binding buffer using the aptamer probe S4F-based cancer cell detection strategy (B).

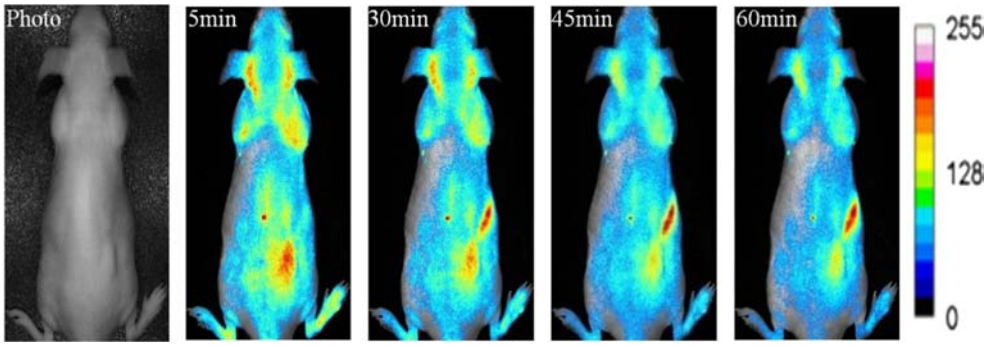

Fig. 5. In vivo specific fluorescence imaging of the SGC7901 tumor with the fluorescent aptamer probe S4F (Cy5-S4F-BHQ2). The aptamer probe was injected into the SGC7901 tumor-bearing mouse. Fluorescent images of the dorsal side of gastric tumor bearing mice were taken within 15 min postinjection time. Time of exposure for every fluorescent image was 1000 ms, and the pink circles locate the tumor site. (For interpretation of the references to color in this figure legend, the reader is referred to the web version of this article.)

target cells were released from FMNS after 40 min enzyme digestion. This further demonstrated our selected aptamers hold great potential in gastric cancer diagnosis and might be used to capture CTC s in the clinical samples.

Before the in vivo experiment, flow cytometry assays were performed to investigate the fluorescence activation of the fluorescent aptamer probes by target cancer cells. Here, aptamer S1a, S1b, S2a and S4a was coupled with FAM group at the 5′end and quencher group BHQ1 at the 3′ end to design aptamer probes of S1F, S2F, S3Fand S4F. As shown in Fig. 4A, in the absence of targets (incubated with control GES-1 cells), none of the aptamer probes showed elevated fluorescence. In contrast, the fluorescence intensity of the aptamer probes was increased by incubation with target SGC7901 cells, and the fluorescence signal was almost completely recovered. This finding indicated that the aptamer probes were substantially activated by binding to membrane proteins or molecules expressed on the target cancer cells.

In order to further investigate the sensitivity of the fluorescent aptamer probe for detection of SGC7901 cells, samples with varying SGC7901 cell numbers ranging from 300 to 300,000 in 200 μL binding buffer were obtained by serial dilution. The aptamer S4a was chosen as a model to be modified as follows: Cy5-GATCTCTCTCTGCCCTAAGTCCGCACCCGTGCTTCCCTGT-BHQ2. To quantify the target cell number, statistical analyses were performed according to the aptamer probe-labeled events appearing in the upright (UR) region. As shown in Fig. 4B, as the cell number decreased, the number of events located in the UR region decreased accordingly. At the lowest cell number (300), we detected a signal in the UR region. These results indicated that our aptamer probe was sensitive to the target cells and hold great promise as a good molecular probe for cancer diagnosis.

To further validate the imaging specificity, the ability of the aptamer probe to target the SGC7901 tumor-bearing mice was tested in vivo. The aptamer probe S4F was chosen as a model: Cy5-GATCTCTCTCTGCCCTAAGTCCGCACCCGTGCTTCCCTGT-BHQ2. SGC7901 tumor-bearing mice received intravenous injection of 1.5 nmol labeled probe with 4.5 nmol unlabelled, unselected oligonucleotide. As we expected, the aptamer probe circulated rapidly throughout the animal within 15 min, and clear fluorescence signals could be observed in most parts of the body, including the tumor site. As displayed in Fig. 5, within15 min, the aptamer probe was enriched in the SGC7901 tumor-implanted site and a clearly enhanced fluorescence signal was observed at the over time, the aptamer was circulated into the kidney, but this observation preliminarily demonstrated that our selected aptamer had great potential to be used to detect gastric tumor cells.

4. Conclusions

In summary, our results demonstrated that using cell-SELEX strategy, the selected aptamers could specifically recognize human gastric tumor tissues compared to the normal tissues. When the selected aptamers were conjugated with fluorescent-magnetic nanospheres (FMNS) to capture cancer cells, they showed high captured and release efficiency. The newly designed aptamer probe underwent a conformational change upon binding to the target cancer cell, which resulted in the activation of a fluorescence signal. Flow cytometry assays revealed that the aptamer probe was specifically activated by the target cancer cells and showed high sensitivity for SGC7901 cells. Furthermore, the aptamer probe was able to specifically target the SGC7901 tumor site and exhibited a very bright fluorescence signal within 15 min after injection. The aptamer probe strategy hold a great potential to design molecular probes for in vivo cancer imaging with high sensitivity and specificity.

Acknowledgements

Zhou and Zhang thanks the National Basic Research Program of China (973 Program) (2012CB720600, 2012CB720603, 2012CB720604), the National Science Foundation of China (Nos. 91213302, 81025008, 31221061) the National Grand Program on Key Infectious Disease (2012ZX10003002-014, 2012ZX10003002-015) and Program for Changjiang Scholars and Innovative Research Team in University (IRT1030). We thank Lingling Gong, Zhongnan Hospital of Wuhan University, helping to detect tissues.

Appendix A. Supporting information

Supplementary data associated with this article can be found in the online version at http://dx.doi.org/10.1016/j.talanta.2014.09.036.

References

[1] G.A. Soukup, G.A. Emilsson, R.R. Breaker, J. Mol. Biol. 4 (2000) 623–632.
[2] Z. Tang, D. Shangguan, K. Wang, H. Shi, K. Sefah, P. Mallikratchy, H.W. Chen, Y. Li, W. Tan, Anal. Chem. 13 (2007) 4900–4907.
[3] R. Nutiu, Y. Li, Angew. Chem. Int. Ed. Engl. 7 (2005) 1061–1065.
[4] D. Shangguan, Y. Li, Z. Tang, Z.C. Cao, H.W. Chen, P. Mallikaratchy, K. Sefah, C. J. Yang, W. Tan, Proc. Natl. Acad. Sci. U.S.A 32 (2006) 11838–11843.
[5] S.M. Shamah, J.M. Healy, S.T. Cload, Acc. Chem. Res. 1 (2008) 130–138.
[6] S. Bi, B. Ji, Z. Zhang, S. Zhang, Chem. Commun. (Cambridge) 33 (2013) 3452–3454.
[7] M.N. Ara, M. Hyodo, N. Ohga, K. Hida, H. Harashima, PLoS One 12 (2012) e50174.
[8] K. Sefah, D. Shangguan, X. Xiong, M.B. O'Donoghue, W. Tan, Nat. Protoc. 6 (2010) 1169–1185.

[9] J.K. Herr, J.E. Smith, C.D. Medley, D. Shangguan, W. Tan, Anal. Chem. 9 (2006) 2918–2924.
[10] Y. Wan, Y.T. Kim, N. Li, S.K. Cho, R. Bachoo, A.D. Ellington, S.M. Iqbal, Cancer Res. 22 (2010) 9371–9380.
[11] B. Guven, A.N. Basaran, E. Temur, U. Tamer, I.H. Boyaci, Analyst 136 (2011) 740–748.
[12] J. Baniukevic, I.H. Boyaci, A.G. Bozkurt, U. Tamer, A. Ramanavicius, A. Ramanaviciene., Biosens. Bioelectron. 43 (2013) 281–288.
[13] X. Fang, A. Sen, M. Vicens, W. Tan, Chem Bio Chem. 4 (2003) 829–834.
[14] C.J. Yang, S. Jockusch, M. Vicens, N.J. Turro, W. Tan, Proc. Natl. Acad. Sci. U.S.A 102 (2005) 17278–17283.
[15] K. Guo, H.P. Wendel, L. Scheideler, G. Ziemer, A.M. Scheule, J. Cell. Mol. Med. 9 (2005) 731–736.
[16] N.K. Navani, Y. Li, Curr. Opin. Chem. Biol. 10 (2006) 272–281.
[17] J.E. Smith, C.D. Medley, Z. Tang, D. Shangguan, C. Lofton, W. Tan, Anal. Chem. 8 (2007) 3075–3082.
[18] D. Shangguan, Z.C. Cao, Y. Li, W. Tan, Clin. Chem. 6 (2007) 1153–1155.
[19] Z. Xiao, D. Shangguan, Z. Cao, X. Fang, W. Tan, Chemistry 6 (2008) 1769–1775.
[20] D. Deng, D. Zhang, Y. Li, S. Achilefu, Y. Gu, Biosens. Bioelectron. 49 (2013) 216–221.
[21] Z.Z. Li, Y.W. Han, L.L. Liu, Y.P. Han, Y. Lu, C.X. Wang, Biotechnology 19 (2009) 42–46.
[22] G.K. Kouassi, P. Wang, S. Sreevatan, J. Irudayaraj, Biotechnol. Prog. 23 (2007) 1239–1244.
[23] H. Shi, Z. Tang, Y. Kim, H. Nie, Y.F. Huang, X. He, K. Deng, K. Wang, W. Tan, Chem. Asian J. 5 (2010) 2209–2213.
[24] T. Jiang, E.S. Olson, Q.T. Nguyen, M. Roy, P.A. Jennings, R.Y. Tsien, Proc. Natl. Acad. Sci. U.S.A 101 (2004) 17867–17872.
[25] G. Blum, G. von Degenfeld, M.J. Merchant, H.M. Blau, M. Bogyo, Nat. Chem. Biol. 3 (2007) 668–677.
[26] M. Ogawa, N. Kosaka, P.L. Choyke, H. Kobayashi, ACS Chem. Biol. 4 (2009) 535–536.
[27] M. Ogawa, N. Kosaka, M.R. Longmire, Y. Urano, P.L. Choyke, H. Kobayashi, Mol. Pharmacol. 6 (2009) 386–395.
[28] H. Shi, X. He, K. Wang, X. Wu, X. Ye, Q. Guo, W. Tan, Z. Qing, X. Yang, B. Zhou, Proc. Natl. Acad. Sci. U.S.A. 108 (2011) 3900–3905.
[29] H.Y. Xie, C. Zuo, Y. Liu, Z.L. Zhang, D.W. Pang, X.L. Li, J.P. Gong, C. Dickinson, W. Zhou, Small 5 (2005) 506–509.
[30] S. Sun, H. Zeng, J. Am. Chem. Soc. 28 (2002) 8204–8205.
[31] X. Fang, W. Tan, Acc. Chem. Res. 1 (2010) 48–63.
[32] D. Shangguan, Z. Tang, P. Mallikaratchy, Z. Xiao, W. Tan, ChemBioChem 6 (2007) 603–606.